We are IntechOpen, the world's leading publisher of Open Access books Built by scientists, for scientists

4,800
Open access books available

122,000
International authors and editors

135M
Downloads

Our authors are among the

154
Countries delivered to

TOP 1%
most cited scientists

12.2%
Contributors from top 500 universities

CLARIVATE ANALYTICS BOOK CITATION INDEX INDEXED

WEB OF SCIENCE™

Selection of our books indexed in the Book Citation Index in Web of Science™ Core Collection (BKCI)

Interested in publishing with us?
Contact book.department@intechopen.com

Numbers displayed above are based on latest data collected.
For more information visit www.intechopen.com

11

Synthesis and Characterization of Ordered Mesoporous Silica Pillared Clay with HPW Heteropoly Acid Encapsulated into the Framework and Its Catalytic Performance for Deep Oxidative Desulfurization of Fuels

Baoshan Li[1], Zhenxing Liu[1], Jianjun Liu[1], Zhiyuan Zhou[2], Xiaohui Gao[2], Xinmei Pang[2] and Huiting Sheng[1]
[1]*State Key Laboratory of Chemical Resource Engineering*
Beijing University of Chemical Technology
[2]*Petrochina Petrochemical Research Institute*
P. R. China

1. Introduction

Because of the increasing environmental concern and legal requirements, it has been an urgent subject to find new processes for ultra-deep desulfurization of fuel oils. The conventional hydrodesulfurization (HDS) technique has some inherent problems in treating sulfur-containing aromatic hydrocarbon compounds, such as dibenzothiophene (DBT) and its derivatives. Thus, a large number of non-HDS processes, such as adsorption, extraction, oxidation, precipitation and bio-processes have been explored [1-7]. Among these methods, catalytic oxidative desulfurization (ODS) combined with extraction is regarded as the most promising and economical process [8-11]. The ODS process has been studied in various systems, including oxidant H_2O_2 with inorganic acids [12], organic acids [13-15], TS-1 [16], and heteropoly acids (HPA) catalysts [17-19]. HPA catalysts, especially those having the Keggin structure, have been determined to be very effective for the oxidation of sulfur-containing compounds in a liquid-liquid two-phase system. However, the separation and recovery of the catalysts are very difficult. For these reasons, the stable and water-tolerant solid acid catalysts have been developed. Li et al. [20], Lü et al. [21], and Gao et al. [22] reported $[(C_{18}H_{37})_2N(CH_3)_2]_3[PW_{12}O_{40}]$, $[C_{18}H_{37}N(CH_3)_3]_4[H_2NaPW_{10}O_{36}]$, and $Q[W(O)(O_2)_2(C_5H_4NCO_2)]$ ($Q=(C_4H_9)_4N$, $[(CH_3)_3N(C_{18}H_{37})]$ and $[(C_{18}H_{37})_2N(CH_3)_2]$) catalysts, respectively. Over these catalysts, DBT and its derivatives can be selectively oxidized into their corresponding sulfones using H_2O_2 as the oxidant in diesel oil. The surfactant-type catalysts provided a new process for deep ODS. However, the double long carbon chains of quaternary ammonium surfactant used in their system are very expensive.

In our previous works, monovacant lacunary Keggin-type polyoxometalate was introduced into mesoporous silica structure and showed high oxidation activity for ODS [23]. Furthermore, we recently prepared a series of ordered mesoporous clay materials known as silica pillared clay (SPC) materials and metal ion doped SPC materials [24-29]. These

inorganic porous materials with a controlled pore structure have stimulated a great deal of interest for their potential application as selective catalysts, adsorbents, separating agents, and porous matrixes for encapsulation of specific functional molecules [30-33].
In this study, in order to combine the porous advantages of the SPC and the appropriate acidity of $H_3PW_{12}O_{40}$ (HPW) heteropoly acid, HPW was encapsulated into the ordered mesoporous SPC material by sol-gel method (denoted as HPW-SPC-SG) involving introduction of the HPW into clay interlayer template in an acidic suspension. The catalytic performance of the HPW-SPC-SG materials was studied through the ODS of the model oil. The results indicate that the HPW-SPC-SG materials exhibited high catalytic performance in ODS.

2. Experimental

2.1 Materials

All solvents and reactants are commercially available and were used without further purification. The natural montmorillonite clay (MMT) was obtained from Inner Mongolia and used as the starting clay without any further purification or ions exchanging. The raw clay had a basal (001) spacing of 15.4 Å and an anhydrous structural (layer) formula of $[Si_{7.86}Al_{0.14}][Al_{2.84}Fe_{0.30}Mg_{0.86}]O_{20}(OH)_4$, with a cation exchange capacity (CEC) of 91 meq/100 g [24].

2.2 Preparation

2.0 g of MMT was first suspended in 120 mL of deionized water in a round bottom flask, to which 4.0 g of cetyltrimethylammonium bromide (CTAB) dissolved in 10.0 mL of pure ethanol was added dropwise and stirred for 1 h and a gel mixture was gained. Then, the pH of the gel was adjusted by HCl solution to 2.0. Subsequently, the calculated amount of $H_3PW_{12}O_{40}.6H_2O$ was dissolved in 10.0 mL of water and added dropwise into the prepared gel under vigorous stirring. After the mixture was stirred for 4 h, 10.0 mL of tetraethyl orthosilicate (TEOS) was added, followed by stirring for 12 h at room temperature. And then, the mixture was put into an autoclave and heated for 24 h in a furnace at 110 ^oC. The autoclave was cooled, and the product was separated by filtration, throughly washed with deioined water, and dried in an oven at 110 ^oC. Then the dried samples were calcined at 500 ^oC for 6 h in a furnace. The samples were designated as x%HPW-SPC-SG (where x% represents the weight percentage of HPW in the samples), and analyzed by X-ray fluorescence analysis (XRF). The results show that the actual content of HPW are 6.65, 13.24, and 24.93 wt.% for the samples with nominal HPW content of 5, 15 and 25 wt.%, respectively.
The SPC sample was prepared following the same procedure as the HPW-SPC-SG samples without the addition of HPW. And the impregnated samples were also prepared by an incipient wetness impregnation method using SPC as the support [34-36]. The loading amount of HPW was varied in the range of 5 to 25 wt.% by changing the concentration of the HPW in water. Typically, an aqueous HPW solution volume of 5 ml was used per gram of freshly calcined SPC. After impregnation, the wet samples were dried at 110 oC in an oven. The final HPW/SPC samples prepared by impregnation were denoted as x%HPW-SPC-IM, where x% also represents weight percentage of HPW in the samples.

2.3 Catalytic performance in oxidative desulphurization

The model compound DBT was dissolved into *n*-octane to make a stock solution of model oil with sulfur content of 500 ppm. The reaction was performed in a three-neck glass flask with a water-bathed jacket. The mixture of the model oil (25 mL) and the catalyst (0.15 g) was heated under vigorous stirring. When the required reaction temperature was reached, 0.12 mL of 30% aqueous solution of H_2O_2 ($n_{H_2O_2}/n_S$=3) was added into the reactor under stirring for a certain time. Then the oxidized model oil was extracted three times by acetonitrile, and the volume ratio of the total solvent to model oil was 1:1. The amount of sulfur in the oil was determined by a Model WK-2D microcoulometric integrated analyzer (sulfur detection range from 0.2-5000 ppm, Jiangsu Jiang Fen Electroanalytical Instrument Co.).

2.4 Characterization

X-ray diffraction was performed on a Rigaku D/Max 2500 VBZ+/PC diffractometer using Cu-Kα radiation at low-angle range (2θ value 0.5°-10°) and at wide-angle range (2θ value 3°-70°). XRF was performed on a Philips Magix-601 X-ray fluorescence spectrometer. Thermogravimetric and differential thermal analysis (TGDTA) was carried out on a HCT-1 thermal analyzer (Hengjiu Kexue Co.) using a heating rate of 10 °C min^{-1}. The FT-IR spectra were obtained in KBr pellets using a Bruker VECTOR 22 spectrometer in the range of 400-4000 cm^{-1}, and all spectra were collected at room temperature with a resolution of 4 cm-1. Nitrogen adsorption isotherms were obtained using a Micromeritics UNCALCINEDAP 2000 instrument. The samples were degassed at 115 °C for 8 h before the measurement. The specific surface area (S_{BET}) was estimated by the BET equation, and the pore size distribution and the mesopore analysis were obtained from the desorption branch of the isotherm using the Barrett-Joyner-Halenda (BJH) method. The scanning electron microscopy (SEM) micrographs were obtained on a Hitachi S-4700 microscope operated at 30 kV.

3. Results and discussion

3.1 The formation mechanism of the HPW-SPC-SG samples

Scheme 1 illustrates the proposed formation mechanism of the HPW-SPC-SG materials. Firstly, MMT was suspended in aqueous solutions and ion-exchanged with surfactant CTAB. During this process, the surfactant formed micelle in the interlayer regions. Then, the pH of the mixture was adjusted by HCl solution to 2.0 and an appropriate amount of HPW was introduced into the solution. $PW_{12}O_{40}^{3-}$ can substitute Br^- and Cl^- in the shell surrounding the micelle. Furthermore, the addition of HCl solution can keep the solution in a strong acidic environment to retain the Keggin-type HPW heteropoly acid intact. When TEOS was finally added into the gel mixture, it would intercalate into the clay interlayer regions by solvation and rapidly hydrolyze in acidic conditions to form the protonated $H_5SiO_4^+$ monomers. The silicate cations would interact with the anionic shell surrounding the CTAB micelle to trap both X^- (Cl^-, Br^-) and heteropoly anions, leading to the formation of a silica layer around the surfactant template. Thus, the heteropoly anions would be present at the interface between the silica and the CTAB micelle. During the long time stirring and hydrothermal treatment of the gel, the silica layer was polymerized and formed the Si-O-Si bonds between the interlayer regions. Washing and drying steps did not remove the heteropoly anions since they were trapped inside the clay interlayer. In the calcination step, the silica layer further condensed and yielded the completely cross-linked framework to

strengthen the siloxanepillars and the mesopore structure, while the CTAB template decomposed and was eliminated from the pore system, but the HPW molecules remained fixed into the SPC frameworks [37].

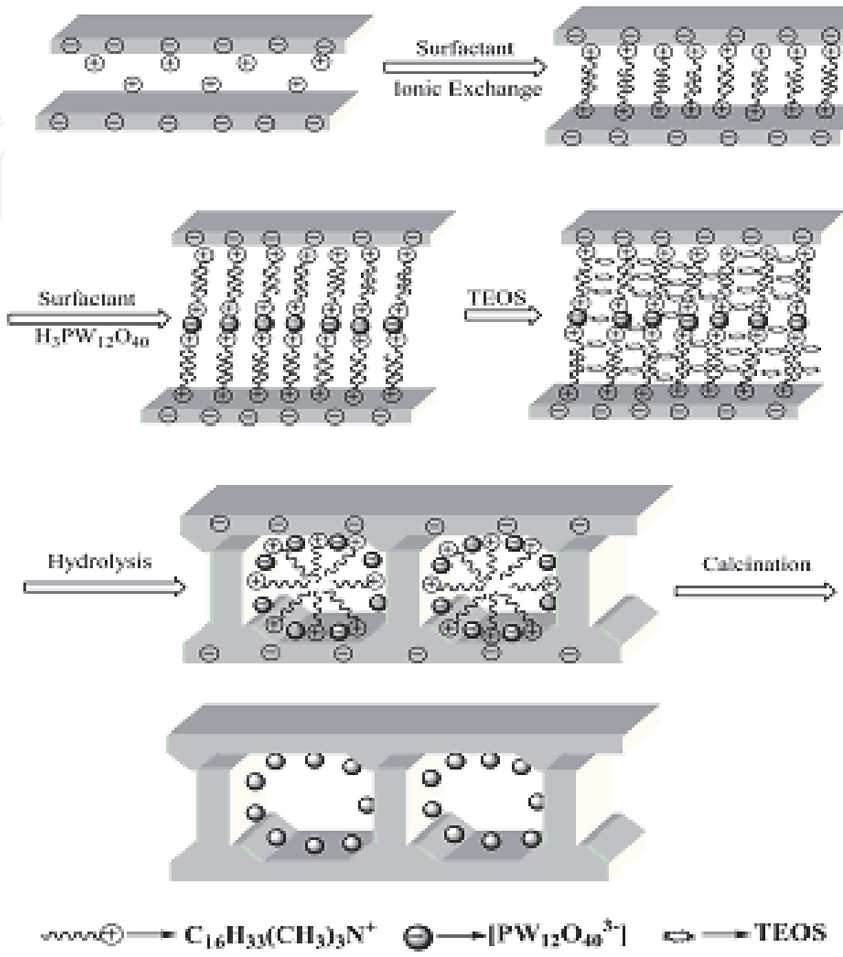

Scheme 1. Formation mechanism of the HPW-SPC-SG samples

3.2 The characterization of the samples

The small angle XRD patterns of the calcined MMT, SPC and HPW-SPC-SG samples are shown in Figure 1A. All the HPW-SPC-SG samples showed a broad characteristic (001) diffraction peak at about 2.0, which indicates that introducing HPW during the intercalation of CTAB did not destroy the SPC mesoporous lamellar structure. This result supports the proposed formation mechanism of the HPW-SPC-SG samples. The basal spacing and the gallery height of HPW-SPC-SG samples are summarized in Table 1. The HPW-SPC-SG materials exhibited refraction corresponding to a basal spacing of 4.38-4.47 nm. Since the thickness of the clay layer sheet is about 0.96 nm [38], the corresponding gallery heights are around 3.42-3.51 nm. Moreover, with theincrease of the HPW content, the refraction peak shifted to the low angle scope and the gallery height was found to increase gradually. This implies that the HPW has been encapsulated into the silica pillared frameworks of the SPC.

However, with the introduction of more HPW, the XRD peaks became less resolved, as the 25%HPW-SPC-SG sample gave no obvious diffraction peak. This is because that the HPW is encapsulated into the SPC frameworks, while the excessive amount of HPW clog the pore passages [39].

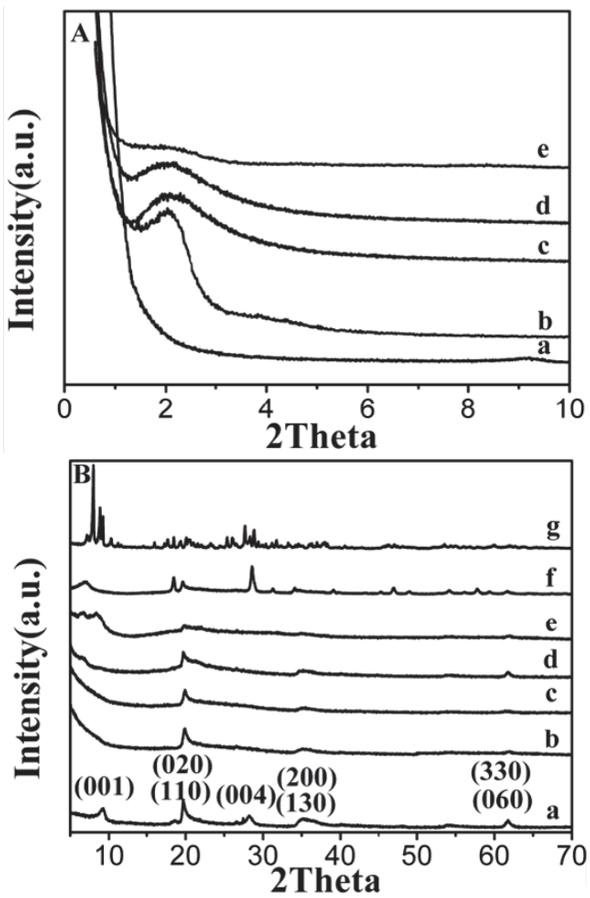

Fig. 1. A. Low-angle XRD patterns of samples: (a) calcined MMT, (b) SPC, (c) 5%HPW-SPC-SG, (d) 15%HPW-SPC-SG, and (e)25%HPW-SPC-SG.
B. Wide-angle XRD patterns of samples: (a) calcined MMT, (b) SPC, (c) 5%HPW-SPC-SG, (d) 15%HPW-SPC-SG, (e) 25%HPW-SPC-SG, (f) 15%HPW-SPC-IM, and (g) pure HPW.

The wide angle XRD patterns of the calcined MMT, SPC, HPW-SPC-SG, 15%HPW-SPC-IM and HPW samples are presented in Figure 1B. The SPC and the HPW-SPC-SG samples all showed the MMT characteristic peaks, which were assigned to (110), (020), (004), (130), (200), (330) and (060) diffractions [29, 40]. This ulteriorly approves that the laminated structure of MMT and the crystalline structure of the clay sheet have not been destroyed during the intercalation of HPW. However, with the increase of the HPW content, the HPW-SPC-SG samples gradually showed some characteristic peaks of HPW crystal, which was obvious for the 25%HPW-SPC-SG sample. The phenomenon indicates that the excess amount of HPW was introduced into the interlayer, but the HPW was not highly dispersed in the mesoporous SPC [41, 42]. On the other hand, the characteristic peaks of HPW in the pattern of 15%HPW-SPC-IM sample can be evidently seen. The results indicate that HPW is

much more highly dispersed in the HPW-SPC-SG samples than that in the HPW-SPC-IM samples.

The TG-DTA curves of the SPC, HPW and HPW-SPC-SG samples before calcination in the region of 30-800 °C are shown in Figure 2. For all the samples, the weight loss below 100 °C was attributed to the loss of the physisorbed H_2O. There was a weight loss peak in the range of 210-500 °C for the SPC sample (Figure 2a), which was due to the decomposition of CTAB in the sample. The corresponding DTA curve indicated that CTAB template elimination was associated with a sharp exothermic peak centered at 323 °C [43]. Another endothermic peak in the DTA diagram centered at 706 °C was corresponding to the collapse of the mesoporous gallery structure [44].

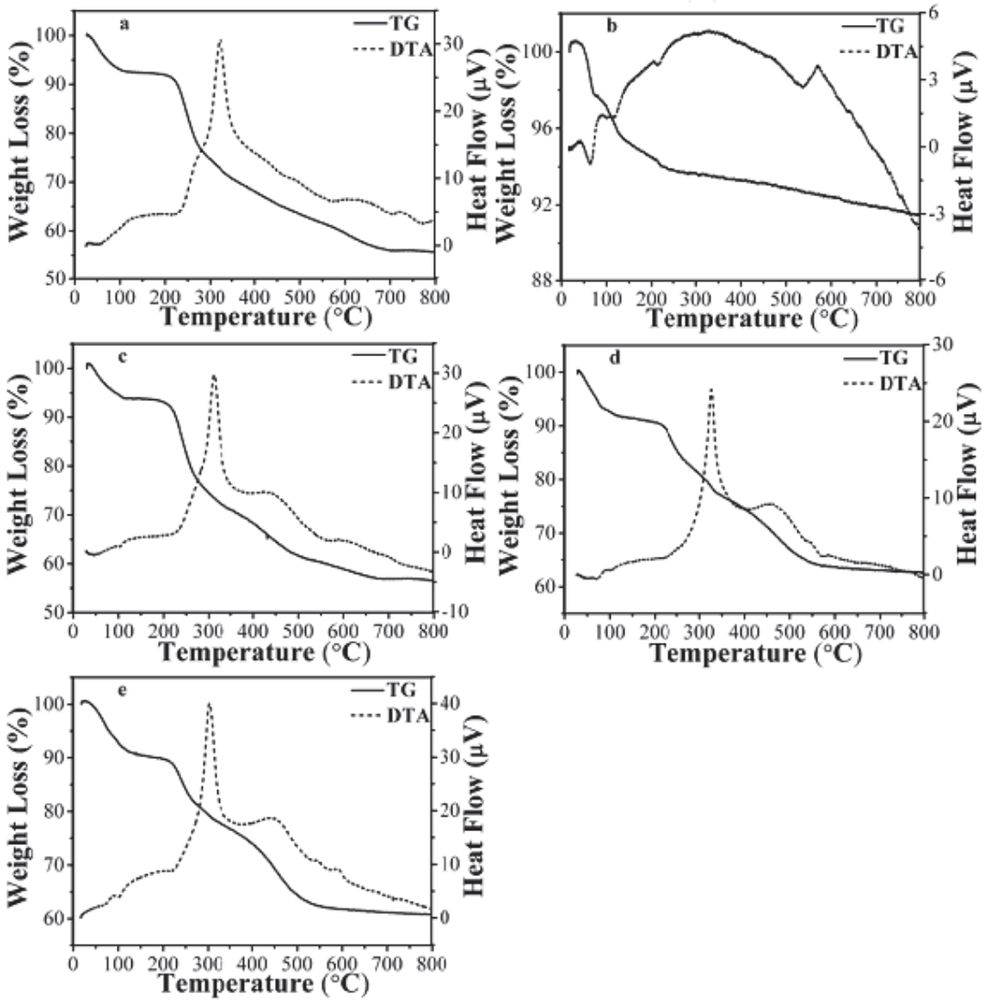

Fig. 2. TG-DTA curves of samples (a) SPC, (b) pure HPW, (c) 5%HPW-SPC-SG, (d) 15%HPW-SPC-SG, and (e) 25%HPW-SPC-SG

For the pure HPW (Figure 2b), there was an endothermic peak in the temperature range of 100-320 °C(weight loss 3.57%) centered at 215 °C in the DTA diagram, accounting for the loss of 6 H_2O molecules per Keggin unit of the HPW. The endothermic peak also appeared in the DTA diagrams of the HPW-SPC-SG samples (Figure 2c, d, e). The exothermic peak of HPW

beginning at 538 °C in the DTA curve is assigned to the decomposition of heteropoly acid to form mixed oxides [45, 46]. The appreciable exothermic peak was also observed between 538-592 °C in the DTA diagrams of the HPW-SPC-SG samples (Figure 2c, d, e), indicating that the HPW-SPC-SG materials did not lower the thermal stability of the HPW heteropoly acid.

For the HPW-SPC-SG samples, besides the exothermic peaks at 323 °C, there was another exothermic peak centered at 407 °C in the DTA diagram (Figure 2c, d, e), which was also attributed to the decomposition of CTAB [47]. The decomposition of the organic cation extending to a higher temperature was due to the interactions of the CTAB and the HPW. Furthermore, the endothermic peak corresponding to the collapse of the mesoporous gallery structure also appeared in the DTA diagram of the HPW-SPC-SG samples (Figure 2c, d, e). This implies that the incorporation of the HPW did not destroy the interlayer gallery structures of the HPW-SPC-SG samples. The TG-DTA curves also show that the HPW-SPC-SG samples can be obtained after treating the gels at 500 °C for 6h.

The FT-IR spectra of the pure HPW, SPC and HPW-SPC-SG samples in the region of 1400-600 cm^{-1} are shown in Figure 3. The spectrum of the HPW showed a broadened band at 802 cm^{-1}, which was assigned to *v*as (W-Oc-W) in edge shared octahedral [48]. The spectrum of SPC showed a band at 795 cm^{-1}, which was attributed to the symmetric stretching frequency of Si-O-Si [49]. In FT-IR spectrum of HPW-SPC-SG, the peak was shifted to 816 cm^{-1}, which was due to the chemical interactions between HPW and SPC. As reported by Hu et al [50], the band at 816 cm^{-1} was attributed to the formation of Si-O-W bonds. Therefore, we can conclude that the HPW was encapsulated into the mesoporous silica framework and formed new Si-O-W bonds within the silica wall of the SPC material, which is consistent with the proposed formation mechanism of the HPW-SPC-SG samples. The characteristic bands of Keggin-type HPW were also observed at 1080, 980 and 890 cm^{-1}, which are usually assigned to *v*as(P-O), *v*as(W=O), and *v*as(W-Ob-W) in corner shared octahedral [48], respectively. Moreover, in the FT-IR spectra of HPW-SPC-SG samples, especially of the 25%HPW-SPC-SG sample, these bands were evidently strengthened compared to the bands of SPC, which further indicates the encapsulation of HPW in the SPC frameworks [51].

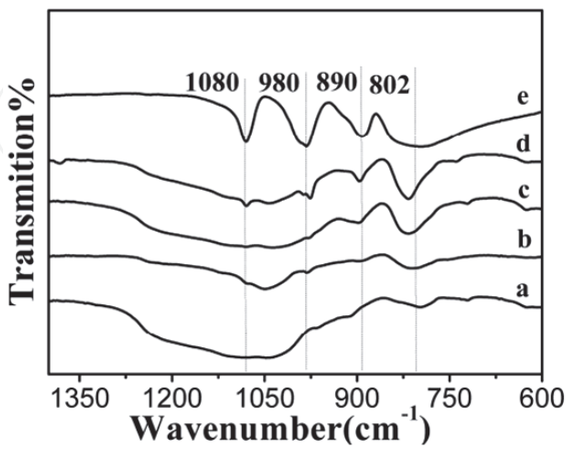

Fig. 3. FT-IR spectra of the samples: (a) SPC, (b) 5%HPW-SPC-SG, (c) 15%HPW-SPC-SG, (d) 25%HPW-SPC-SG, and (e) pure HPW.

The nitrogen adsorption/desorption isotherms and the mesoporous size distribution of the HPW-SPC-SG samples are shown in Figure 4. All samples presented type IV isotherm patterns with H3-type hysteresis loop starting at about 0.4 partial pressure, which are the characteristics of the mesoporous materials with the cylindrical pores formed in gallery regions [52]. For the 25%HPW-SPC-SG sample, the hysteresis loop of the isotherm was obviously smaller than that of the samples with relatively low HPW contents. Furthermore, the desorption branch of the sample extended to a relatively lower pressure, suggesting a partial loss of structural organization and the formation of some narrower slit-shaped pores [37]. Nevertheless, the main part of the hysterese was still between *P/P0* values of 0.50-0.95. The data shown in Table 1 demonstrate that the S_{BET} of the HPW-SPC-SG samples are about 324-444 $m^2\ g^{-1}$, which are lower than that of the SPC (538 $m^2\ g^{-1}$), but much higher than that of the HPW-SPC-IM samples (148-170 $m^2\ g^{-1}$) and the MMT (80 $m^2\ g^{-1}$). The results in Table 1 also indicate that the total pore volume (V_T) of the HPW-SPC-SG samples are slight lower than that of the SPC sample, but much higher than that of the HPW-SPC-IM samples and the MMT. The significant loss of S_{BET} and V_T of the HPW-SPC-IM samples can be related to the agglomeration of HPW molecules on the external surface of the materials resulting in pore blockage [36, 46]. The S_{BET} and V_T almost linear decreased with the increase of the HPW content both in the HPW-SPC-SG and the HPW-SPC-IM samples, which is logical since the heteropoly acid contributes to the sample weight.

The mesoporous pore size distribution is depicted in the inset of Figure 4. The results also indicate that all the HPW-SPC-SG samples have about the same pore diameters around 4.46-4.52 nm, which are slightly smaller than that of the SPC sample (5.06 nm). In the sol-gel synthesis method, the size of the majority of mesopores is formed by the CTAB micelle and the interclayer space, which is affected scarcely by the presence of HPW. This is in agreement with the proposed formation mechanism (Scheme 1). On the contrary, the pore diameters of the HPM-SPC-IM samples are reduced to about 4.33-3.82 nm, which indicates that HPW inside the mesopores occupied the space and decreases the pore width [37].

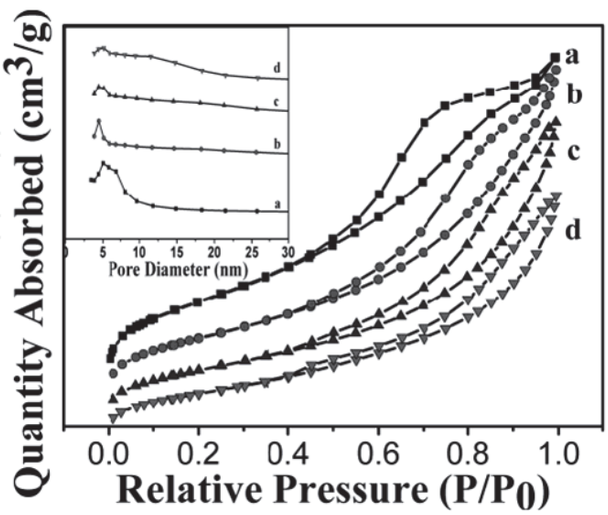

Fig. 4. Nitrogen adsorption/desorption isotherms and pore size distribution curves of samples: (a) SPC, (b) 5%HPW-SPC-SG, (c)15%HPW-SPC-SG, and (d) 25%HPW-SPC-SG.

Catalysts	Pore size[a] (nm)	S_{BET} ($m^2 \cdot g^{-1}$)	Basal spacing (nm)	Gallery height[b] (nm)	V_T ($cm^3 \cdot g^{-1}$)
MMT	4.30	64	1.54	0.58	0.14
SPC (0%HPW)	5.06	538	4.35	3.39	0.79
5%HPW-SPC-SG	4.46	444	4.38	3.42	0.73
15%HPW-SPC-SG	4.46	377	4.43	3.47	0.64
25%HPW-SPC-SG	4.52	324	4.47	3.51	0.51
5%HPW-SPC-IM	4.33	170	4.35	3.39	0.48
15%HPW-SPC-IM	3.86	152	4.35	3.39	0.44
25%HPW-SPC-IM	3.82	148	4.35	3.39	0.43

[a] The values were determined from N_2 desorption isotherm.
[b] The gallery height is defined as basal spacing minus the 0.96 nm thickness of MMT layer.

Table 1. Textural properties of MMT, SPC, HPW-SPC-SG and HPW-SPC-IM samples

The SEM images of the SPC, HPW-SPC-SG and 15%HPW-SPC-IM samples are shown in Figure 5. The SPC sample exhibited a slightly swelled nature mortmorillite plates morphology [27], while all the HPW-SPC-SG samples also exhibited plates structure, which was similar to the morphologies of the SPC sample. Though there were more fragmental particles with the increase of the HPW content in the HPW-SPC-SG samples, the main laminated structures of the HPW-SPC-SG samples were still retained, which indicates that the interlayer gallery structures were unaffected by the incorporation of the HPW. The 15 wt.% HPW-SPC-IM sample also retained a mortmorillite lamellar structure, though the HPW has an impact on the surface of the lamellar structure.

3.3 Catalytic performance of oxidizing modle oil

The effect of the reaction time on the ODS of the modle oil with sulfur content of 500 ppm over the HPW-SPC-SG catalysts is shown in Figure 6. It is obvious that the sulfur removal over 5%HPW-SPC-SG, 15%HPW-SPC-SG and 25%HPW-SPC-SG catalysts can reach up to 97.6%, 97.8% and 95.8% within 80 min, respectively. The results indicate that the HPW-SPC-SG samples are highly efficient in catalytic ODS of the DBT. But the 25%HPW-SPC-SG sample exhibited comparatively lower activity than the 15%HPW-SPC-SG sample, this is because the presence of high HPW contents leads to the decrease of the *S*BET of the 25%HPW-SPC-SG sample (Table 1). With the increase of the reaction time, the sulfur removal of the samples was remarkably raised in 80 min, and just slightly increased after 80 min. For the 15%HPW-SPC-SG sample, the sulfur content can be reduced to 7.2 ppm within 100 min.

The sulfur removal of the model oil over the 15%HPW-SPC-SG catalyst with reaction time at different temperatures is shown in Figure 7. The sulfur removal appeared to be unsatisfying at a temperature of 40 °C, which may be because H_2O_2 and the catalyst cannot work efficiently under low reaction temperature. Raising the reaction temperature from 40 to 60 °C led to a remarkable increase in the sulfur removal. However, further increase of the reaction temperature to 70 °C caused the decrease of the desulfurization efficiency. This is because the high temperature leads to the partial decomposition of H_2O_2, which brings down the oxidation effeciency. But the sulfur removal at 70 °C was still higher than that at 50 °C, which indicates that a proper increase of temperature favores the ODS of DBT.

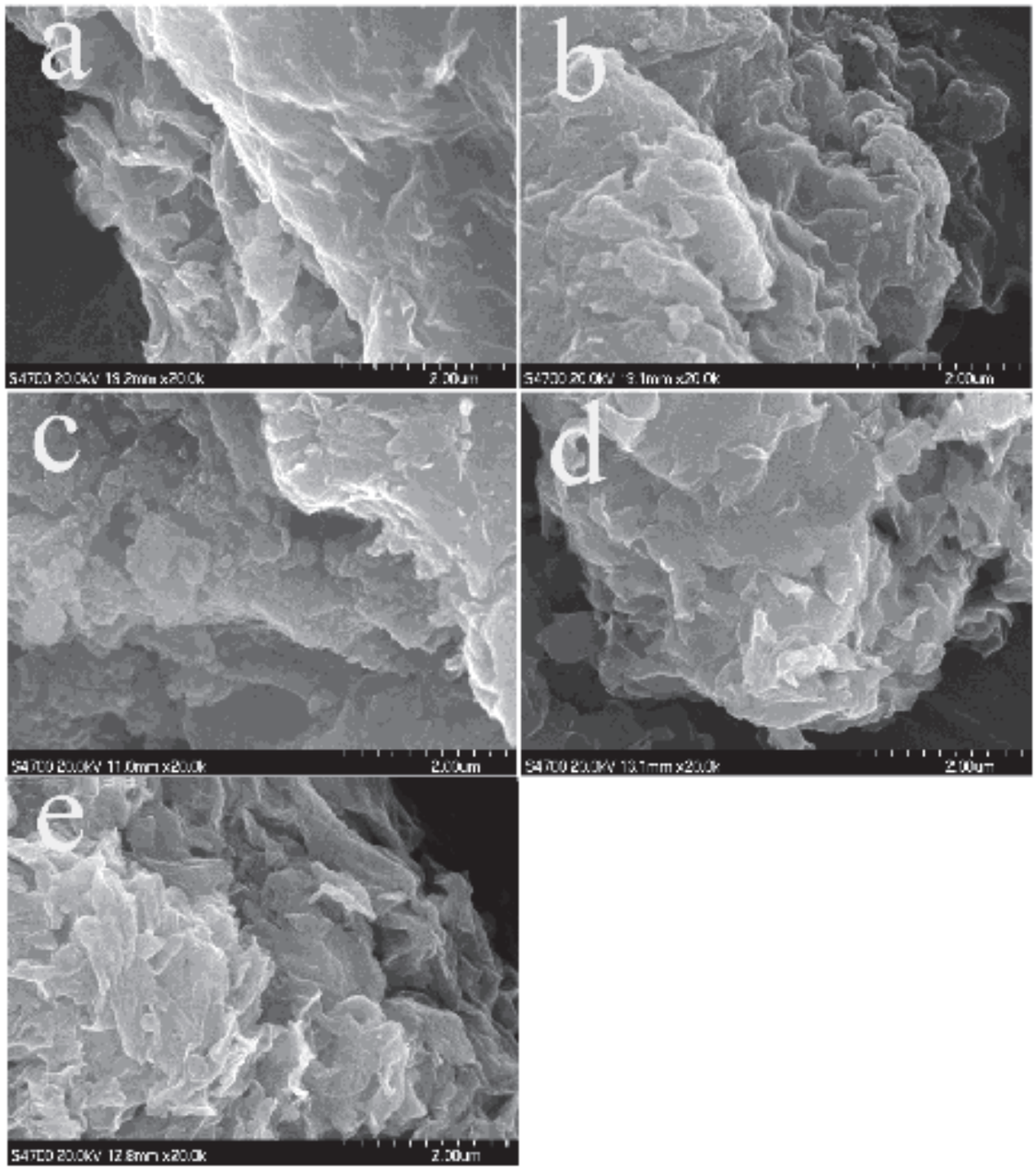

Fig. 5. SEM images of samples: (a) SPC, (b) 5%HPW-SPC-SG, (c) 15%HPW-SPC-SG, (d) 25%HPW-SPC-SG, and (e) 15%HPW-SPCIM.

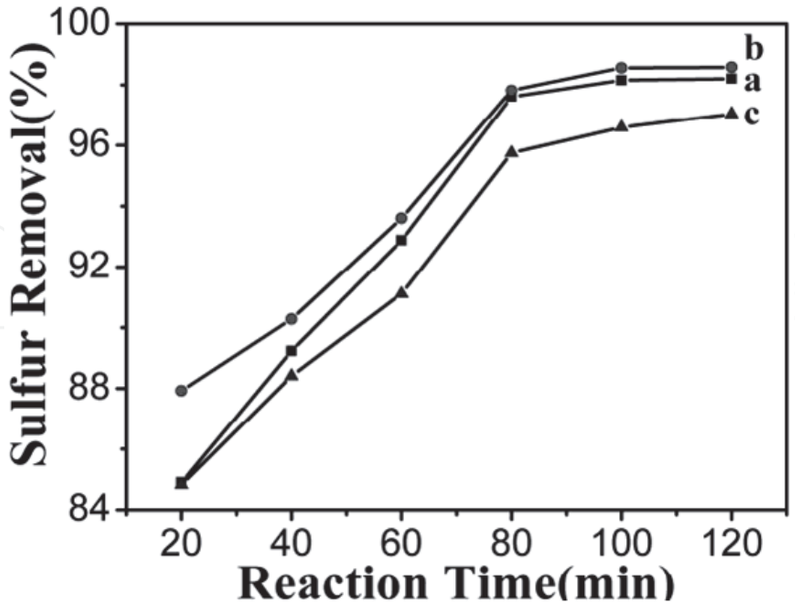

Fig. 6. Effect of reaction time on ODS of samples: (a) 5%HPW-SPC-SG, (b) 15%HPW-SPC-SG, and (c) 25%HPW-SPC-SG. Reaction temperature is 60 oC.

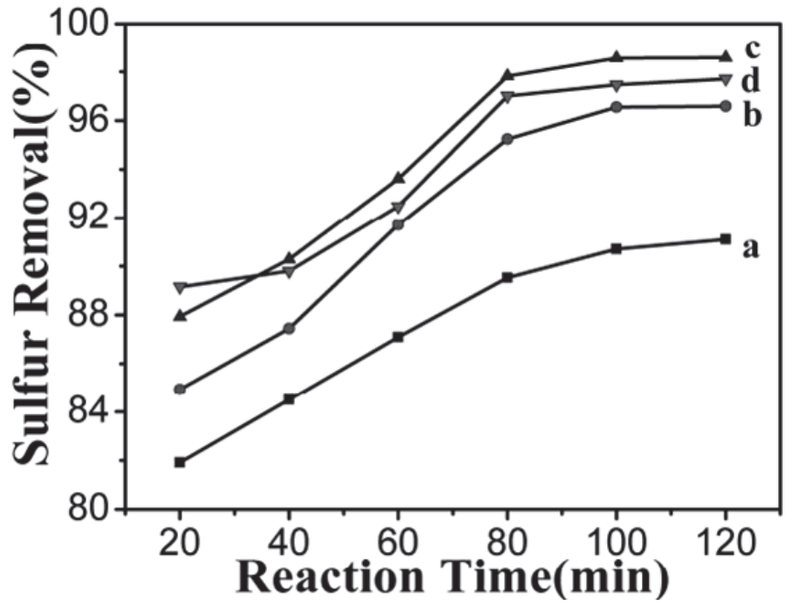

Fig. 7. Effect of reaction time and temperature on ODS: (a) 40 °C, (b) 50 °C, (c) 60 °C, and (d) 70 °C.

Table 2 shows the results of the sulfur removal of the model oil over different catalysts. The results indicated that direct extraction without oxidation resulted in lower sulfur removal. And the catalytic activity of the HPW-SPC-SG samples was better than that of the HPW-SPC-IM samples. This is because the *S*BET and pore size of the HPW-SPC-SG samples are

much bigger than that of the HPW-SPC-IM samples. On the other hand, HPW has been encapulated into the silica pillared frameworks of SPC in the HPW-SPC-SG samples, which leads to the better stability and continuous catalytic ability of HPW.

Catalysts	S remaining (E)[a] (ppm)	S remaining (ppm)	S removal (%)
-	177.3	174.1	65.2
SPC (0% HPW)	154.3	148.8	70.2
5%HPW-SPC-SG	161.8	9.0	98.2
15%HPW-SPC-SG	164.2	7.1	98.6
25%HPW-SPC-SG	169.2	14.8	97.0
5%HPW-SPC-IM	168.3	146.7	70.7
15%HPW-SPC-IM	170.4	131.7	73.7
25%HPW-SPC-IM	173.0	116.9	76.6

a (E) means the extraction results of the samples without oxidation. Reaction temperature is 60 oC and reaction time is 120 min.

Table 2. Catalytic performance of SPC, HPW-SPC-SG, and HPW-SPC-IM catalysts

4. Conclusions

The HPW-SPC-SG materials were successfully prepared by sol-gel method. The catalysts showed a homogeneous dispersion of the HPW molecules even at 25 wt.% loading. HPW was encapsulated into the gallery silica framework structure in the HPW-SPC-SG samples. The HPW-SPC-SG materials showed better catalytic performance for ODS of the oil than that of the HPW-SPC-IM samples. Under the optimized conditions, the sulfur content in the model oil can be reduced from 500 to 7.1 ppm. The prepared HPW-SPC-SG materials are promising and efficient catalysts for ODS of fuel oils.

5. Acknowledgements

The work was financially supported by the National Basic Research Program of China (973 Program, Grant No. 2011CBA00506).

6. References

[1] R. T. Yang, A. J. Hernández-Maldonado, F. H. Yang, Science 301 (2003) 79.
[2] H. Tao, T. Nakazato, S. Sato, Fuel 88 (2009) 1961.
[3] Y. Shiraishi, K. Tachibana, T. Hirai, I. Komasawa, Ind. Eng. Chem. Res. 41 (2002) 4362.
[4] S. Murata, K. Murata, K. Kidena, M. Nomura, Energy Fuels 18 (2004) 116.
[5] I. V. Babich, J. A. Moulijn, Fuel 82 (2003) 607.
[6] E. Ito, J. A. Rob van Veen, Catal. Today 116 (2006) 446.
[7] C. Song, X. Ma, Appl. Catal. B: Environ. 41 (2003) 207.
[8] A. K. Sharipov, V. R. Nigmatullin, Pet. Chem. 45 (2005) 371.
[9] A. Sharipov, V. Nigmatullin, I. Nigmatullin, R. Zakirov, Fuels Oils 42 (2006) 451.
[10] A. Anisimov, A. Tarakanova, Russ. J. Gen. Chem. 79 (2009) 1264.

[11] J. M. Campos-Martin, M. C. Capel-Sanchez, P. Perez-Presas, J. L. G. Fierro, J. Chem. Technol. Biotechnol. 85 (2010) 879.
[12] P. S. Tam, J. R. Kittrell, J. W. Eldridge, Ind. Eng. Chem. Res. 29 (1990) 321.
[13] G. X. Yu, S. X. Lu, H. Chen, Z. Zhu, Carbon 43 (2005) 2285.
[14] F. Al-Shahrani, T. C. Xiao, S. A. Llewellyn, S. Barri, Z. Jiang, H. H. Shi, G. Martinie, M. L. H. Green, Appl. Catal. B: Environ. 73 (2007) 311.
[15] P. D. Filippis, M. Scarsella, Energy Fuels 17 (2003) 1452.
[16] L. Y. Kong, G. Li, X. S. Wang, B. Wu, Energy Fuels 20 (2006) 896.
[17] M. Te, C. Fairbridge, Z. Ring, Appl. Catal. A: Gen. 219 (2001) 267.
[18] H. M. Li, L. N. He, J. D. Lu, W. S. Zhu, X. Jiang, Y. Wang, Y. S. Yan, Energy Fuels 23 (2009) 1354.
[19] M. Arias, D. Laurenti, C. Geantet, M. Vrinat, I. Hideyuki, Y. Yoshimura, Catal. Today 130 (2008) 190.
[20] C. Li, Z. Jiang, J. Gao, Y. Yang, S. Wang, F. Tian, F. Sun, X. Sun, P. Ying, C. Han, Chem. Eur. J. 10 (2004) 2277.
[21] H. Y. Lü, J. Gao, Z. X. Jiang, F. Jing, Y. X. Yang, G. Wang, C. Li, J. Catal. 239 (2006) 369.
[22] J. B. Gao, S. G. Wang, Z. X. Jiang, H. Y. Lu, Y. X. Yang, F. Jing, C. Li, J. Mol. Catal. A: Chem. 258 (2006)261.
[23] Z. E. A. Abdalla, B.S. Li, A. Tufail, Colloids Surf. A: Physicochem. Eng. Aspects 341 (2009) 86.
[24] H. H. Mao, B. S. Li, X. Li, Z. X. Liu, W. Ma, Appl. Surf. Sci. 255 (2009) 4787.
[25] B. S. Li, H. H. Mao, X. Li, W. Ma, Z. X. Liu, J. Collid. Interface. Sci. 336 (2009) 244.
[26] H. H. Mao, B. S. Li, X. Li, Z. X. Liu, W. Ma, Mater. Res. Bull. 44 (2009) 1569.
[27] H. H. Mao, B. S. Li, X. Li, Z. X. Liu, W. Ma, Catal. Commun. 10 (2009) 975.
[28] H. H. Mao, B. S. Li, X. Li, L. W. Yue, Z. X. Liu, W. Ma, Ind. Eng. Chem. Res. 49 (2010) 583.
[29] H. H. Mao, B. S. Li, X. Li, L. W. Yue, Micropor. Mesopor. Mater. 130 (2010) 314.
[30] H. Ishida, S. Campbell, J. Blackwell, Chem. Mater. 12 (2000) 1260.
[31] R. A. Horch, T. D. Golden, N. A. D'Souza, L. Riester, Chem. Mater. 14 (2002) 3531.
[32] H. Y. Zhu, J. C. Zhao, J. W. Liu, X. Z. Yang, Y. N. Shen, Chem. Mater. 18 (2006) 3993.
[33] J. C. Juan, J. C. Zhang, M. A. Yarmo, J. Mol. Catal. A: Chem. 267 (2007) 265.
[34] A. Miyaji, T. Echizen, K. Nagata, Y. Yoshinaga, T. Okuhara, J. Mol. Catal. A: Chem. 201 (2003) 145.
[35] T. Sugii, R. Ohnishi, J. Zhang, A. Miyaji, Y. Kamiya, T. Okuhara, Catal. Today 116 (2006) 179.
[36] Q. H. Xia, K. Hidajat, S. Kawi, J. Catal. 209 (2002) 433.
[37] B. C. Gagea, Y. Lorgouiloux, Y. Altintas, P. A. Jacobs, J. A. Martens, J. Catal. 265 (2009) 99.
[38] M. Pluta, A. Galeski, M. Alexandre, M.-A. Paul, P. Dubois, J. Appl. Polym. Sci. 86 (2002) 1497.
[39] J. Toufaily, M. Soulard, J. L. Guth, J. Patarin, L. Delmote, T. Hamieh, M. Kodeih, D. Naoufal, H. Hamad, Colloids Surf. A: Physicochem. Eng. Aspects 316 (2008) 285.
[40] S. Bracco, P. Valsesia, L. Ferretti, P. Sozzani, M. Mauri, A. Comotti, Micropor. Mesopor. Mater. 107 (2008)102.
[41] A. Ghanbari-Siahkali, A. Philippou, J. Dwyer, M. W. Anderson, Appl. Catal. A: Gen. 192 (2000) 57.

[42] Á. Kukovecz, Zs. Balogi, Z. Kónya, M. Tobab, P. Lentzc, S. I. Niwa, F. Mizukami, Á. Molnárd, J. B. Nagyc, I. Kiricsi, Appl. Catal. A: Gen. 228 (2002) 83.
[43] F. Kleitz, W. Schmidt, F. Schüth. Micropor. Mesopor. Mater. 65 (2003) 1.
[44] M. L. Occelli, Ind. Eng. Chem. Prod. Res. Dev. 22 (1983) 553.
[45] I. V. Kozhevnikov, J. Mol. Catal. A: Chem. 262 (2007) 86.
[46] S. Ajaikumar, A. Pandurangan, J. Mol. Catal. A: Chem. 286 (2008) 21.
[47] J. A. Gamelas, F. A. S. Couto, M. C. N. TrovaÄo, A. M. V. Cavaleiro, J. A. S. Cavaleiro, J. D. Pedrosa de Jesus, Thermochim. Acta 326 (1999) 165.
[48] C. Rocchiccioli-Deltcheff, M. Foumier, R. Frank, Inorg. Chem. 22 (1983) 207.
[49] H. Y. Zhu, Z. Ding, J. C. Barry, J. Phys. Chem. B 106 (2002) 11420.
[50] L. H. Hu, S. F. Ji, Z. Jiang, H. L. Song, P. Y. Wu, Q. Q. Liu, J. Phys. Chem. C 111 (2007) 15173.
[51] A. Bordoloi, F. Lefebvre, S. B. Halligudi, J. Catal. 247 (2007) 166.
[52] F. Rojas, I. Kornhauser, C. Felipe, J. M. Esparza, S. Cordero, A. Dominguez, J. L. Riccardo, Phys. Chem. Chem. Phys. 4 (2002) 2346.

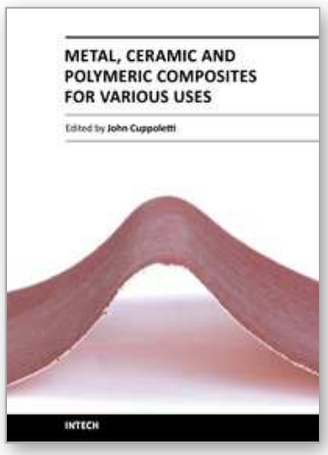

Metal, Ceramic and Polymeric Composites for Various Uses

Edited by Dr. John Cuppoletti

ISBN 978-953-307-353-8

Hard cover, 684 pages

Publisher InTech

Published online 20, July, 2011

Published in print edition July, 2011

Composite materials, often shortened to composites, are engineered or naturally occurring materials made from two or more constituent materials with significantly different physical or chemical properties which remain separate and distinct at the macroscopic or microscopic scale within the finished structure. The aim of this book is to provide comprehensive reference and text on composite materials and structures. This book will cover aspects of design, production, manufacturing, exploitation and maintenance of composite materials. The scope of the book covers scientific, technological and practical concepts concerning research, development and realization of composites.

InTech Europe

University Campus STeP Ri
Slavka Krautzeka 83/A
51000 Rijeka, Croatia
Phone: +385 (51) 770 447
Fax: +385 (51) 686 166
www.intechopen.com

InTech China

Unit 405, Office Block, Hotel Equatorial Shanghai
No.65, Yan An Road (West), Shanghai, 200040, China
中国上海市延安西路65号上海国际贵都大饭店办公楼405单元
Phone: +86-21-62489820
Fax: +86-21-62489821

IntechOpen